F100 Fan Stall Flutter Problem Review and Solution

James D. Jeffers II* and Carl E. Meece Jr.*
Pratt & Whitney Division, United Aircraft Corporation, West Palm Beach, Fla.

An experimental investigation was conducted to examine an airfoil durability problem in the first fan rotor of the F100 engine. This study incorporated laboratory and simulated engine flight tests, an empirical correlation of aeroelastic stability parameters from engine test data, and substantiation testing of the redesign. The results of this investigation's initial testing showed that rotor failure at high-flight Mach numbers and low altitudes was caused by torsional stall flutter instability. The results of the empirical correlation indicated that a design free of flutter required a decrease in both normalized incidence and reduced velocity. Further, the correlation indicated that the flutter was affected by inlet pressure, a heretofore undocumented phenomenon. The results of the substantiation testing confirmed that the redesign made the rotor flutter-free throughout the entire aircraft flight envelope. It was concluded that an improved stall flutter analysis was required to ensure stable fan and compressor rotor designs. It was further concluded that the effect of changes in inlet pressure level on rotor stability was, in part, the result of the accompanying changes in air density and steady-state aerodynamic loading.

Nomenclature

A = unsteady lift function
b = semichord, ft
B = unsteady moment function
β_1 = relative flow angle
β_{min} = relative flow angle at minimum loss
β_l = relative flow angle at minimum loss plus reference loss
h = dimensionless bending deflection, in semichords
k = $b\omega/U$, reduced frequency
KE = kinetic energy, ft-lb
M = Mach number
n = number of rotor blades
$SLTO$ = sea level take off
U = steady fluid velocity relative to blade, fps
W = unsteady work per cycle, ft-lb
α = twist angle, rad (positive nose up)
δ = logarithmic decrement
θ = phase angle between bending and torsional motions, rad
ρ = air density, lb-sec^2/ft^4
ω = frequency, rad/sec

Subscripts

aero = aerodynamic
h = due to bending
I = imaginary part
R = real part
tot = total
α = due to pitch

Superscripts

$(-)$ = amplitude or average over one cycle

I. Introduction

THE F100 engine is a twin-spool, high thrust-to-weight ratio, turbofan engine developed for the F-15 fighter aircraft. The fan has three rotating stages, each with part-span shrouds as shown in Fig. 1. The original first-stage fan blade, which is located immediately behind a variable inlet guide vane, has a shroud mounted aft of the airfoil midchord at approximately 65% span. Airfoil fatigue failures were discovered in the first rotor after engine testing at simulated high Mach number flight conditions. The multiple circular arc series airfoil was designed for high tip-speed operation, but in the failure region of the flight envelope the outer portion of the airfoil experiences subsonic relative Mach numbers and stalled incidences.

Materials laboratory tests showed that the airfoil failures, a typical example of which is shown in Fig. 2, were high-cycle fatigue cracks caused by a high amplitude response in a predominantly torsional mode of vibration. Both the nature of the failures and the aerodynamic environment of the airfoils at the time of failure indicated the problem could likely have been the result of stall flutter; however, predictions and rig testing earlier in the program had anticipated no aeroelastic problems.

II. Initial Flutter Analysis

The design system used to predict subsonic stall flutter consisted of a stability boundary that was a function of two parameters (Fig. 3). One of the parameters is reduced velocity ($\bar{V} = U/b\omega$), which is the inverse of reduced frequency (k) and an important variable in any stability analysis. The second is denoted as β_{1f}, a normalized incidence parameter defined as:

$$\beta_{1f} = (\beta_{min} - \beta_1)/(\beta_{min} - \beta_l) \quad (1)$$

The flow angles in this expression are determined from cascade loss correlations used to generate "loss buckets."

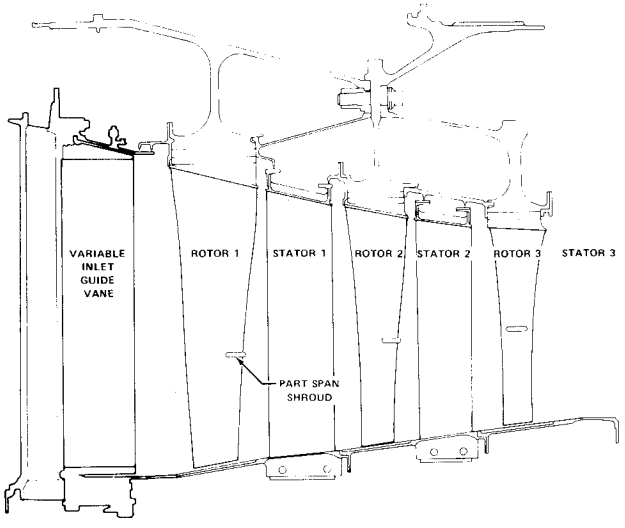

Fig. 1 F100 fan cross section.

Received August 5, 1974. The authors wish to thank the Department of the Air Force, Headquarters Aeronautical Systems Division, Wright-Patterson Air Force Base, Ohio, and the Florida Research and Development Center, Pratt & Whitney Aircraft, Division of United Aircraft Corporation, West Palm Beach, Florida, for permission to publish this paper.

Index categories: Airbreathing Engine Testing; Aeroelasticity and Hydroelasticity.

*Senior Analytical Design Engineer, Florida Research and Development Center.

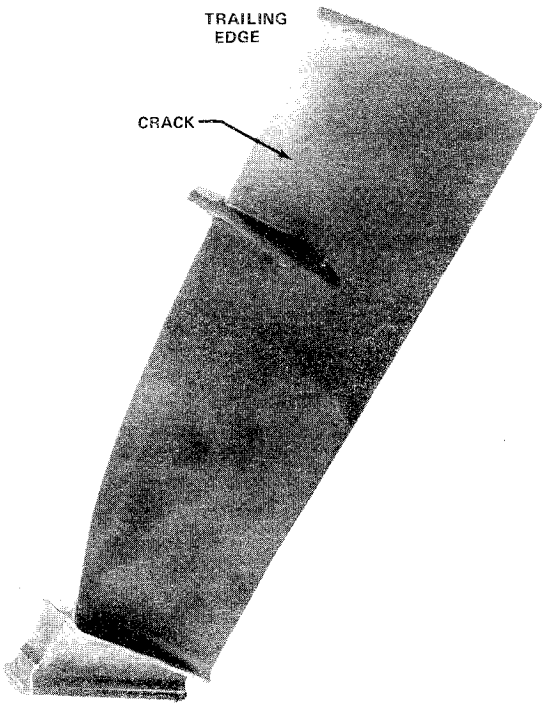

Fig. 2 F100 first-stage airfoil failure.

Thus, β_{1f} is a measure of the flow angle relative to the minimum loss angle on the stalled incidence side of the bucket normalized to account for the incidence range of the airfoil in question. The two-dimensional, bivariate experience limit was generated by enveloping the available stall flutter experience expressed in terms of these variables at a reference span location with a "least stable" flutter boundary (Fig. 3). Obviously, such a system cannot entirely account for 1) many of the two-dimensional, aerodynamic, or structural parameters important to stability analyses or 2) the three-dimensional variations of these parameters. However, the analysis was thought to be conservative and had been effective on earlier designs.

Extensive component testing was conducted early in the development program to evaluate the F100 fan for durability and performance. The testing included heavily instrumented fan rigs that were operated at ambient inlet conditions in sea level test facilities to determine steady-state aerodynamic performance and dynamic structural characteristics for both normal and off-design engine operating conditions.

During the off-design testing of an F100 fan rig, subsonic stall flutter was observed in the first stage at low corrected rotor speed near surge (Fig. 4). The rotor responded in a second-coupled vibratory mode at a frequency of 800 Hz (Fig. 5). The first coupled mode is predominantly bending motion of the blade; the third coupled mode is a torsional mode with most of the motion occurring in the airfoil portion above the partspan shroud. The lower frequency responses of the second coupled mode have a relatively high degree of shroud and disk coupling and the airfoil motion consists primarily of bending. As the second coupled mode frequency increases, the content of torsional motion increases until the mode coalesces into the third coupled, above-shroud-torsion mode. A $\bar{V}$ vs β_{1f} correlation of the rig stall flutter data tended to substantiate the conclusion that the empirical boundary formed a conservative design system (Fig. 6). The rig boundary formed a "nose curve" similar to the correlations of previous Pratt & Whitney Aircraft flutter data at normalized incidences higher than those of the experience limit.

The rig flutter boundary was used to predict the stability of the first fan rotor for an engine at actual flight conditions. The $\bar{V}$ vs β_{1f} limit derived from rig testing was

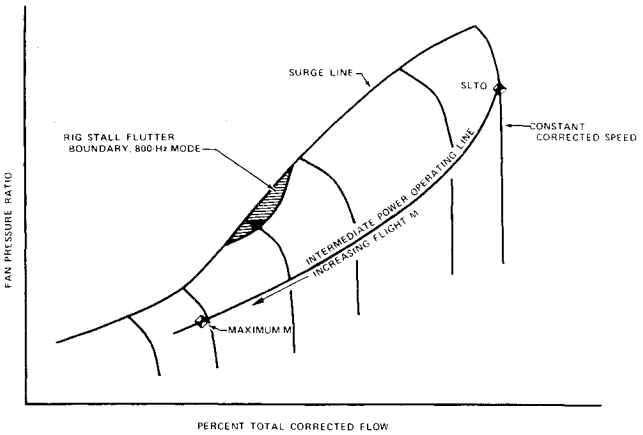

Fig. 4 F100 rig stall flutter fan map.

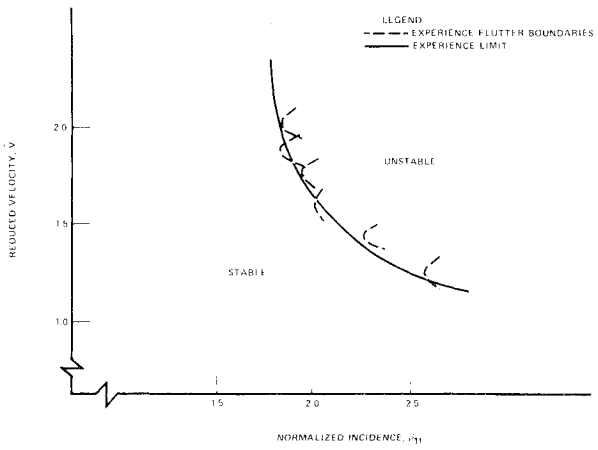

Fig. 3 Torsional stall flutter experience.

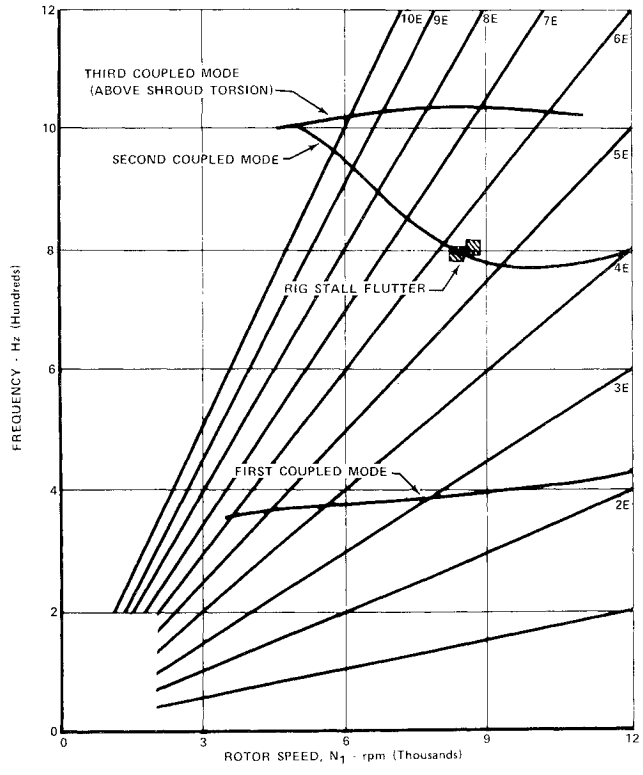

Fig. 5 F100 rig stall flutter resonance diagram.

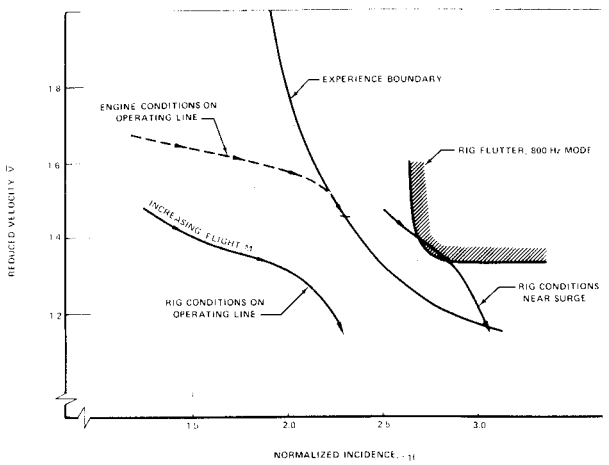

Fig. 6 Prediction of first-stage fan blade stability at engine flight conditions.

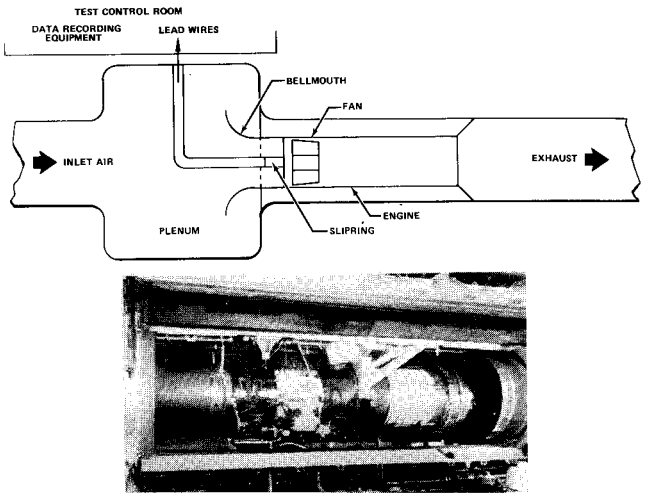

Fig. 8 Altitude test cell.

believed to be more representative because many of the variables unaccounted for in the analysis remain unchanged. Although stalled incidences of the magnitude experienced in the rig at near surge would not be seen by the 1st-stage fan blade during normal engine operation, elevated inlet temperatures were predicted to increase the region of 1st-stage instability (Fig. 6). Increasing inlet temperature increases airfoil relative velocities (fixed relative Mach number) and slightly reduces system natural frequencies for a given operating point. As a result, $\bar{V}$ increases, which is destabilizing relative to the empirical boundary. Inlet temperature does not affect β_{1f} significantly because all the flow velocities change by approximately the same proportion resulting in no relative flow angle change. Inlet pressure level was not expected to affect either $\bar{V}$ or β_{1f} because the velocity triangles remain unchanged and the metal angle changes due to pressure loading were thought to be negligible.

As shown in Fig. 7, the engine was predicted to be free of stall flutter for normal operation at flight conditions. The failures experienced in the F100 engine indicated either the predictions were in error or stall flutter was not the problem.

III. Engine Test Program

A test program was begun to solve the problem. An engine was instrumented and installed in the High Mach Number Test Facility at Pratt & Whitney Aircraft's Florida Research and Development Center (FRDC). The facility has the capability to simulate flight inlet conditions up to and above Mach 3.0 and 70,000 ft altitude. The engine was installed inside a duct; inlet pressure, temperature, and flow environment were completely controlled using slave compressors and exhausters (Fig. 8). Pressure and temperature probes were installed upstream and downstream of the fan to measure aerodynamic performance. Rotating strain gages were applied to selected first-stage blades to measure the vibratory strain and coupled frequency response of the rotor system. The strain gage leadwires were routed to a slipring, which permitted the signals to be transferred from the rotating spool to the stationary FM recording equipment.

Airfoil fatigue failures, similar to those found in the engine, were produced in the materials laboratory by exciting the F100 blade in the above-shroud-torsion, 1000-Hz mode. Figure 9 shows the vibratory strain gage locations employed in the engine to monitor the maximum strains expected to be created by the suspected failure mode and the normal integral order resonant responses. The selection of these locations was based on previous rig experience, laboratory tests, and analytical vibratory mode shape predictions.

An engine test plan was established to investigate the engine flight envelope in the region in which the failures occurred. The approach used to define this region is illustrated through different formats in Fig. 10. Initially, engine inlet conditions were set at a maximum safe experience point based on previous endurance testing (point A). Inlet temperature was then increased to simulate a high Mach number excursion into the failure region of the envelope (point B). Engine scheduling above a certain flight Mach number results in the fan's following a low rotor speed schedule as a function of inlet temperature to ensure aircraft inlet stability. This schedule results in a de-

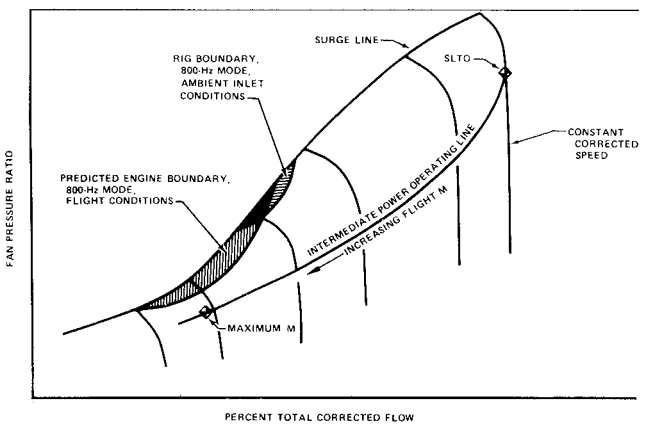

Fig. 7 Predicted stall flutter boundary at engine flight conditions on fan map.

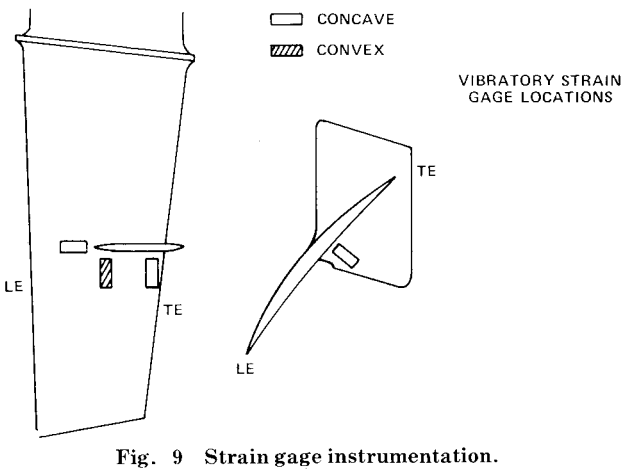

Fig. 9 Strain gage instrumentation.

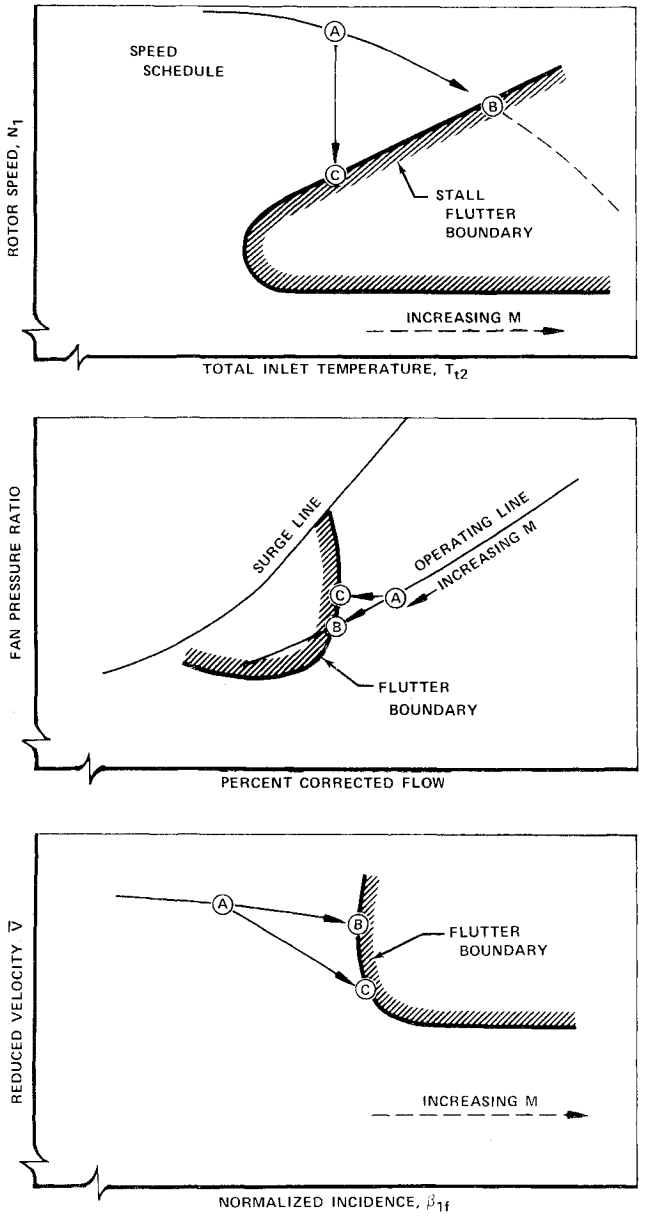

Fig. 10 Engine operation to encounter flutter.

crease in mechanical speed and corrected speed with increasing temperature. Mechanical speed vs total inlet temperature stability limits are an especially convenient means of presentation because these parameters can be accurately measured. They reflect the destabilizing effects on rotor 1 and can be easily monitored by test conductors to avoid problem areas. On a fan map, the fan approaches lower corrected flows and pressure ratios along an operating line as inlet temperature or flight Mach number is increased. During this Mach number transient, rotor 1 experiences increasingly stalled normalized incidence but only slightly decreasing reduced velocities, which is a destabilizing trend relative to the empirical stall flutter experience curve. During testing, inlet temperature was increased until instability was encountered. Flutter onset was also initiated through speed suppression runs. For the suppressed speed excursions, safe steady-state points were set at temperatures well below the flutter region and speed was decreased to encounter flutter (point C). Speed was decreased through a modification of the engine control system that reduced the corrected flow. The fan went down an operating line similar to the one followed on a normal high Mach number transient but at higher pressure ratios and constant temperature. As a result, flutter

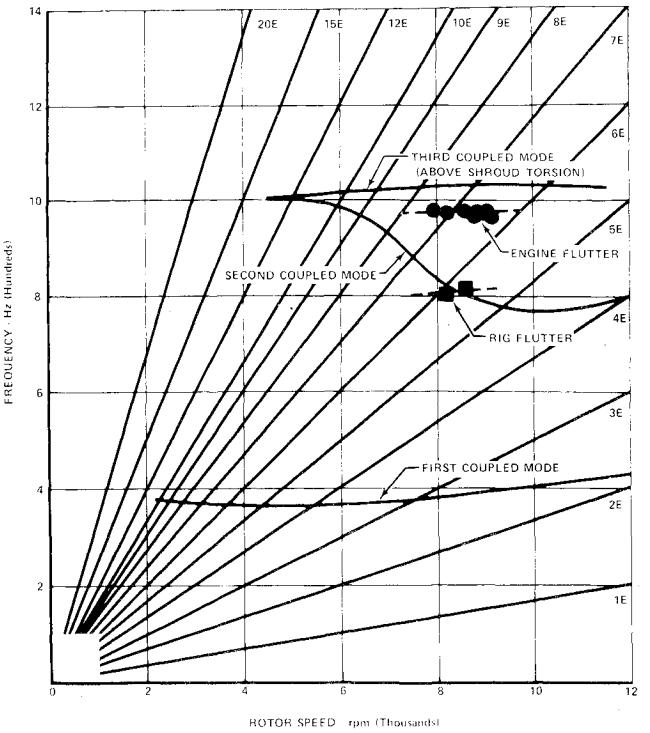

Fig. 11 Rig vs engine stall flutter frequency response.

was generally encountered at higher stalled incidences but lower reduced velocities than on the Mach number transients.

The F100 engine data determined the first stage durability problem was in fact the result of an aeroelastic instability that was a function of stalled incidence. The rotor responded in the above-shroud-torsion mode at a nonintegral order frequency of approximately 1000 Hz as predicted by the laboratory tests. The frequency response was considerably higher than the 800-Hz stall flutter response observed in rig testing (Fig. 11). Although laboratory investigations had indicated the engine would respond in a different mode than the rig, the mechanism causing the change was not understood.

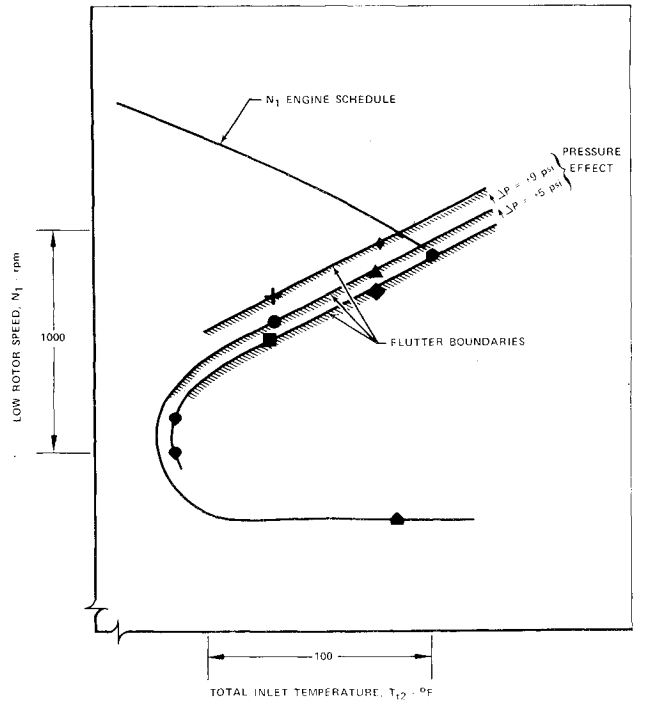

Fig. 12 Stall flutter boundaries from engine tests.

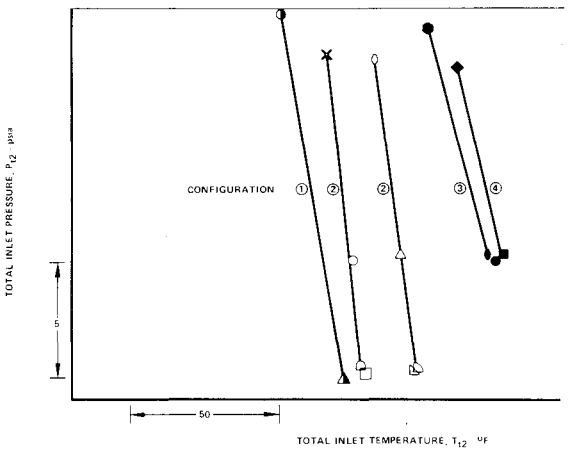

Fig. 13 Inlet pressure vs temperature at flutter inception.

When stall flutter boundaries for the first stage fan blade were generated from engine data points on a speed vs inlet temperature plot, a definite stability dependence on inlet pressure level was observed (Fig. 12). Flutter onset occurred at a lower fan inlet temperature (lower flight Mach number) when inlet pressure was increased. The pressure effect on the onset of flutter observed in the initial F100 test program was later substantiated in stall flutter tests of other configurations. Figure 13 shows total inlet pressure vs total inlet temperature at flutter onset for four different F100 configurations. The data consistently indicate a decrease in system stability with an increase in inlet pressure.

On a fan map, the F100 fan stall flutter boundaries intersected the normal engine operating line away from the predicted engine stall flutter boundary for the 800-Hz rig mode (Fig. 14). A correlation of the engine 1000-Hz stall flutter boundaries on a $\bar{V}$ vs β_{1f} plot is shown in Fig. 15. The F100 rotor 1 flutter was encountered at considerably lower normalized incidences and reduced velocities than in previous Pratt & Whitney Aircraft stall flutter experience.

When rotor 1 was analyzed again at the rig inlet conditions using the engine flutter boundaries, the $\bar{V}$ vs β_{1f} correlation predicted flutter should have been encountered on the rig operating line in the 1000-Hz, above-shroud-torsion mode (Fig. 16). This prediction was in direct conflict with the stability behavior observed in rig testing. As a result of the engine and rig data correlations, the existing stall flutter design system was concluded to be inadequate. However, the general stability trends established by previous experience were concluded still to have validity, i.e., stall flutter stability can be improved by decreasing either reduced velocity or stalled incidence.

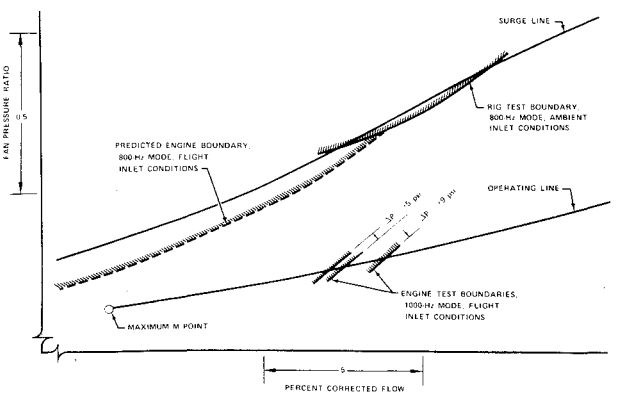

Fig. 14 Stall flutter boundaries on fan map.

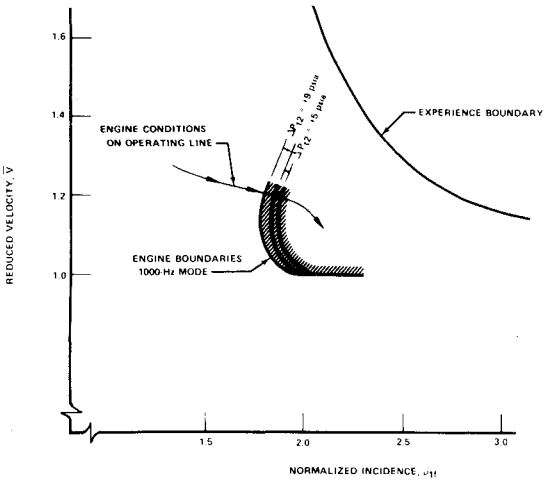

Fig. 15 Empirical correlation of engine stall flutter data.

IV. Solution for Torsional Stall Flutter

The solution to the F100 torsional stall flutter problem was a first-stage blade configuration change. The tip thickness to chord ratio (t/b) was increased from 3 to 5¼%, and the shroud was moved from the trailing edge to the midchord position (Fig. 17). The increased airfoil thickness improved the normalized incidence by improving the blade's loss characteristics (Fig. 18). Because the percentage of thickness increase varied from shroud to tip, the incidence improvement also varied with span location. For the airfoil cross section used to illustrate the loss bucket change, β_{1f} was reduced approximately 30%. The airfoil thickness increase and the movement of the shroud to the midchord position also had a stabilizing effect because the natural frequency of the above-shroud-torsion mode increased. The frequency increased from 1000–1240 Hz causing a corresponding 20% decrease in reduced velocity. The forward movement of the partspan shroud to the midchord position was also believed to have a stabilizing effect based on center-of-twist vs torsional stall flutter stability studies for isolated airfoils of Rainey and Woods.[1,2]

The total effect of the blade configuration changes on the stability of fan rotor 1 was demonstrated in an engine test similar to those used to define the stall flutter problem of the original design. Instrumented engine excursions with the redesigned blade were completed to simulated maximum flight Mach number (maximum inlet temperature) at maximum ram inlet pressure without encountering flutter (Fig. 19). The success of the redesigned

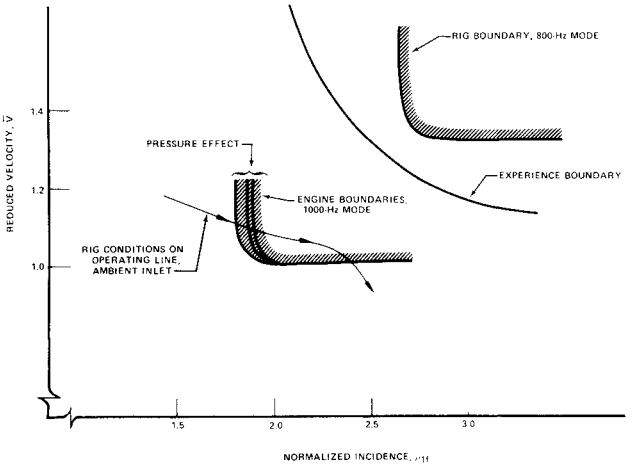

Fig. 16 Empirical stall flutter reanalysis of F100 rotor 1 at rig conditions.

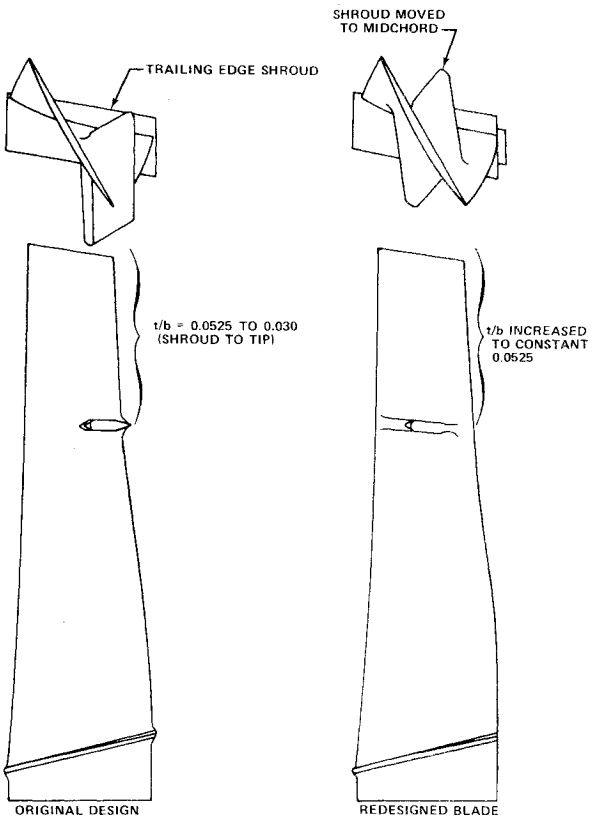

Fig. 17 F100 first-stage fan blade configuration change.

blade is further substantiated by safe flight testing in the F-15 aircraft up to maximum design Mach number without problems.

V Conclusions and Followup

Two basic facts have become apparent as a result of the extensive F100 fan stall flutter test program at FRDC: 1) the existing empirical stall flutter design system could not reliably predict rotor stability for advanced lightweight, high performance fan and compressor designs, and 2) total inlet pressure significantly affects flutter margin.

Shortcomings of Empirical Flutter Prediction Systems

Certain shortcomings of experience-oriented design systems like the two-dimensional, bi-variate stall flutter correlation used in the F100 program have long been recognized. The severity of these shortcomings was not realized until the F100 rotor 1 durability problem was encountered. An effective flutter design system must account for many design parameters and the three-dimensional variations of these parameters, a task virtually impossible to accomplish with an empirical analysis. The energy method of investigating flutter instability used by Carta[3] offers an attractive approach to the establishment of a stall flutter design system. The stability of a system of cascaded airfoils oscillating in uniform steady flow is predicted by calculating the unsteady aerodynamic work per cycle of vibration resulting from the unsteady motion. This approach requires an analytical model to predict the vibratory motion of the blade and a model to generate the unsteady aerodynamic coefficients necessary to calculate the unsteady lift and moment responses. The unsteady work *(W)* is computed by integrating the product of unsteady lift and differential displacement and the product of the unsteady moment and differential twist for one cycle of oscillation. As shown by Carta, the two-dimensional unsteady work can be expressed as follows:

$$W = \rho\pi^2 b^2 U^2 k^2 \{A_{hI}\bar{h}^2 + [(A_{\alpha R} - B_{hR})\sin\Theta + (A_{\alpha I} + B_{hI})\cos\Theta]\bar{\alpha}\bar{h} + B_{\alpha I}\bar{\alpha}^2\} \quad (2)$$

A three-dimensional "strip" analysis can be used to calculate the total blade unsteady work *(W_{tot})* by first performing two-dimensional analyses along the blade span and then integrating from root to tip. A convenient method of comparing the stability of different linear systems is to nondimensionalize the unsteady work per cycle as follows:

$$\delta_{aero} = -(nW_{tot}/4\bar{K}\bar{E}) \quad (3)$$

This quantity is the aerodynamic damping. A similar calculation using the unsteady mechanical work due to frictional forces and material hysteresis yields the mechanical damping. The sum of aerodynamic and mechanical damping is the total system damping. Positive total system damping implies system stability; negative total system damping implies an unstable system (flutter).

Analyses to predict the unsteady motion (natural frequencies and vibratory displacements or mode shapes) are available. Although several theoretical unstalled, unsteady aerodynamic models exist,[4-6] analyses for partially or fully stalled cascaded airfoils at arbitrary incidence angles do not exist and are apparently beyond the state-of-the-art. Recent efforts in aeroelasticity at FRDC have been centered on attempts to modify the theoretical unstalled cascade unsteady aerodynamics that are available to account for high incidences and dynamic stalling. Available experimental data and theoretical models for stalled isolated airfoils were used for the modifications to form a semiempirical stall flutter strip analysis. The abili-

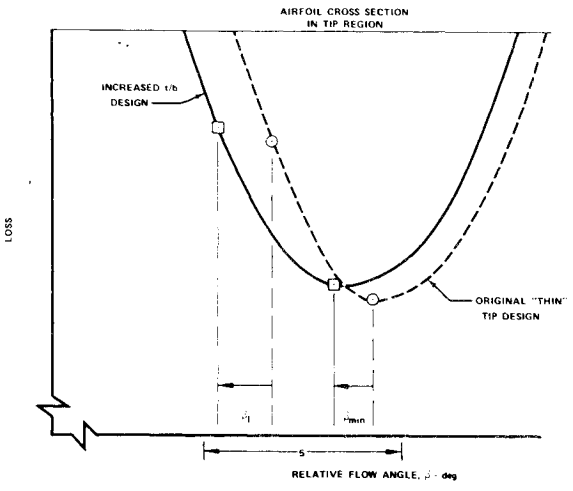

Fig. 18 Improved loss characteristics of redesigned first-stage fan blade.

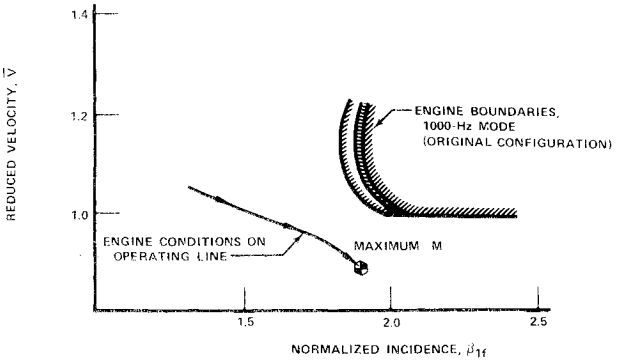

Fig. 19 Redesigned first-stage fan blade stable to maximum Mach number.

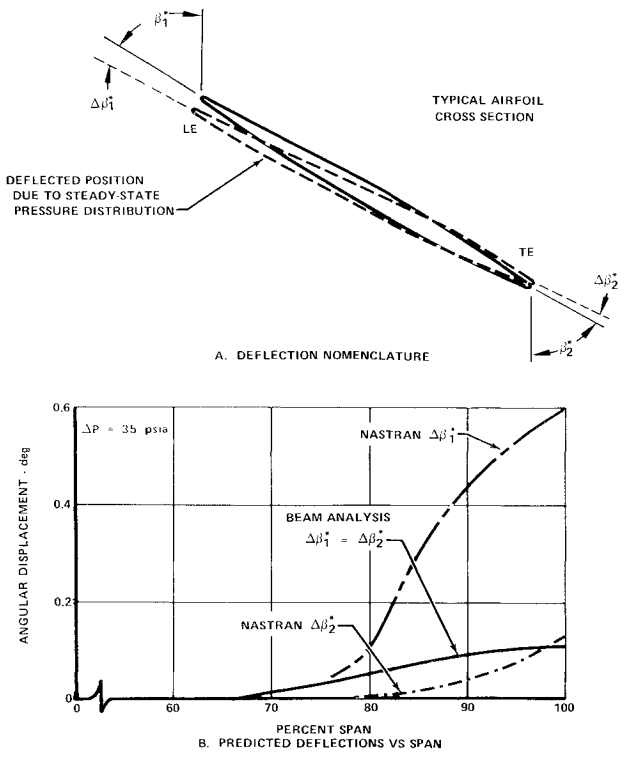

Fig. 20 Predicted pressure effect on cascade geometry.

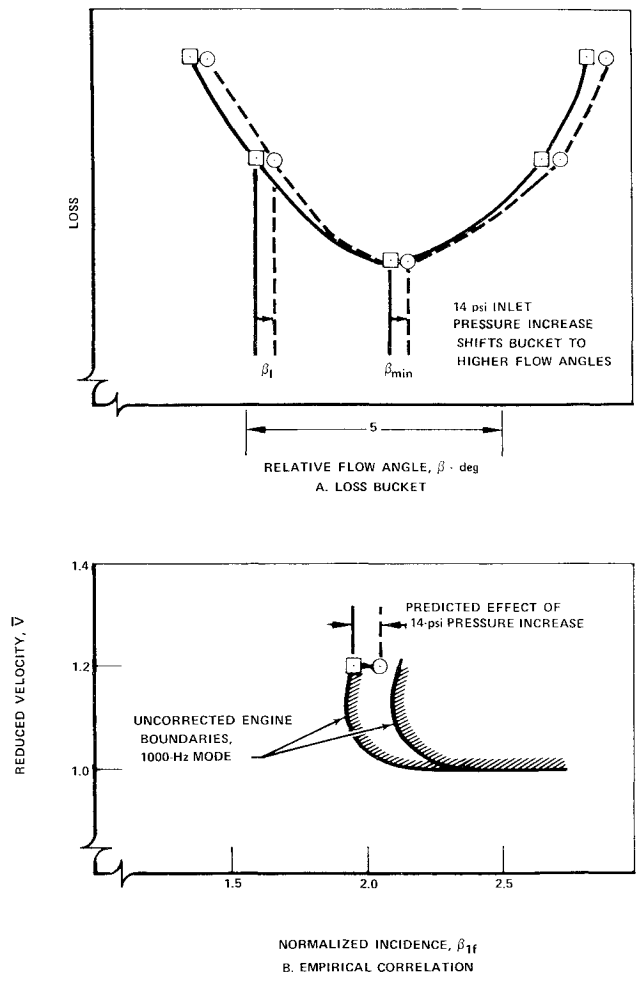

Fig. 21 Predicted pressure effect on airfoil stability.

ty of the system to explain previous stall flutter experience and provide the basis of a more reliable design system is being evaluated. Initial results have been encouraging.

Inlet Pressure Effect

The pressure dependence documented by the F100 engine stall flutter testing cannot fully be explained until an accurate stall flutter design system exists. However, the dependence can qualitatively be explained to be the result of several factors.

For an engine operating at a given inlet temperature, corrected speed, and corrected flow, inlet pressure affects only the density term (ρ) in the unsteady work expression, Eq. (2). Because density is directly proportional to inlet pressure, an increase in pressure produces an increase in the unsteady work and, consequently, the aerodynamic damping. If the system has positive aerodynamic damping, increasing inlet pressure is stabilizing. However, if the aerodynamic damping is negative, increasing inlet pressure is destabilizing. A system that has negative aerodynamic damping can be stable if the positive mechnical damping is large enough to make the total system damping positive. This system can be made unstable at the same operating condition by increasing inlet pressure until the negative aerodynamic damping overcomes the positive mechanical damping.

System stability can be affected by the influence of inlet pressure on cascade geometry. The chordwise pressure distributions created by steady-state aerodynamic loading can cause airfoil chordwise bending and twist deflections that are a direct function of inlet pressure. These deflections affect leading edge metal angle, camber, and cascade stagger. As a consequence, normalized incidence is not only a function of relative flow angle and Mach number but also the changes in cascade geometry resulting from changes in steady-state aerodynamic loading.

The analysis used to determine the effect of aerodynamic loading on incidence in the design phase of the F100 first stage indicated the effect of inlet pressure was negligible. However, this analysis modeled the airfoil as a beam of rigid cross sections and could not determine the chordwise bending deflections. A finite element NASTRAN (NASA Structural Analysis) analysis, performed after the engine tests, predicted the chordwise deflections resulting from pressure loading to be appreciable. The changes in leading and trailing edge metal angles found from each analysis are compared in Fig. 20. The normalized incidence variations predicted for the tip region as a result of the NASTRAN analysis are the same order of magnitude as the β_{1f} changes associated with the pressure induced decreases in stability observed in engine testing (Fig. 21). Thus, at least a portion of the stability dependence on inlet pressure can be explained by airfoil responses to steady-state aerodynamic loading.

An increase in inlet pressure can also have a stabilizing effect by creating an increase in mechanical damping. If relative motion occurs between the two butting faces of the partspan shrouds, frictional work will result that is a function of the normal shroud bearing force generated by the rotational and aerodynamic untwist loads. The NASTRAN analysis predicted the normal force to increase by less than 5% for a 14 psi increase in inlet pressure. Because the majority of the normal force is caused by the centrifugal loading, the increase in positive mechanical damping due to increased pressure should be a second-order effect. Therefore, the increase in stability from the higher shroud loading could not offset the destabilizing trends caused by the density and normalized incidence changes associated with an increase in total inlet pressure.

The stability problem encountered by the F100 first-stage fan rotor has dramatically demonstrated the need to develop a more comprehensive and reliable subsonic

stall flutter design system. Such an analysis must properly account for all the parameters important to aeroelastic stability before durable rotors can be confidently designed with minimum weight and performance penalties. Efforts at Pratt & Whitney Aircraft and the United Aircraft Research Laboratories to provide an accurate and dependable design system have recently been intensified. Major emphasis is being concentrated on developing an energy method of stability analysis. Attempts to generate the unsteady stalled cascade aerodynamics for the analysis include both theoretical investigations and experimental measurement of unsteady lift and moment in an oscillating cascade rig. The blade mode shape prediction is also being improved. NASTRAN is being developed for determining dynamic chordwise deflection, and shroud models are being improved to account more accurately for stiffness and boundary conditions (slippage). The ultimate goal of this work is a system that extends the state-of-the-art to make stall flutter a problem that can be successfully handled during preliminary fan and compressor design.

References

[1]Rainey, A. G. "Preliminary Study of Some Factors which Affect the Stall-Flutter Characteristics of Thin Wings," TN3622, March 1956, Langley Aeronautical Lab., Langley Field, Va., NACA.

[2]Woods, L. C., "Aerodynamic Forces on an Oscillating Aerofoil Fitted With a Spoiler," *Royal Society Proceedings*, New South Wales University of Technology, Ser. A, Vol. 239, 1957, pp. 328–337.

[3]Carta, F. O., "Coupled Blade-Disc-Shroud Flutter Instabilities in Turbojet Engine Rotors," *Winter Annual Meeting and Energy Systems Exposition*, American Society of Mechanical Engineers, Paper 66-WA/GT-6, 1966, pp. 419–426.

[4]Theodorsen, T., "General Theory of Aerodynamic Instability and the Mechanism of Flutter," Rep. 496, 1935, pp. 413–433, NACA.

[5]Whitehead, D.S., "Force and Moment Coefficients for Vibratory Airfoils in Cascade," R. and M. 3254, Feb. 1960, British Aeronautical Research Council, London.

[6]Smith, S. N., "Discrete Frequency Sound Generation in Axial Flow Turbomachines," Rep. CUED/A-Turbo/TR 29, 1971, University of Cambridge, Cambridge, England.

Engineering Note

ENGINEERING NOTES are short manuscripts describing new developments or important results of a preliminary nature. These Notes cannot exceed 6 manuscript pages and 3 figures; a page of text may be substituted for a figure and vice versa. After informal review by the editors, they may be published within a few months of the date of receipt. Style requirements are the same as for regular contributions (see inside back cover).

Modeling of Gas Turbine Engine Compressor Blades For Vibration Analysis

D. A. Anderson*
Wright-Patterson Air Force Base, Ohio

Introduction

THE vibration analysis of gas turbine engine blades is done prior to engine buildup to preclude the possibility of resonance problems in the fundamental modes. Experimental testing is not always feasible especially in the design phase of development as hardware is either nonexistant or unavailable. Several analytical procedures have been developed to predict blade frequencies of which the lumped mass approach and more recently finite element analysis are the most popular. The engineer has the option to choose which method will best suit his needs. The lumped mass approach can give acceptable results using little computer facilities, but only on a special class of blades. Finite element theory on the other hand will give acceptable results on all types of blades, but requires large computer resources and considerable computer time. This paper will examine these two methods of vibration analysis with respect to modeling procedure and validity of results.

Discussion

Vibration analysis using the lumped mass approach is severely limited by the nature of the model. The blade is modeled using chordwise segments lumped to discrete points at the center of the segment. Each segment is considered a point mass and elastic beam with stiffness properties and segment stagger angle taken as constant between masses with these values a representative average of the physical segment. The size of the segments are determined to best simulate the blade by requiring the segment to have relative constant physical geometry. A Holzer-Myklestad approach was used for eigenvalue extraction.

Reference 1 describes the analysis procedure in detail. The idealization this lumped mass approach gives cannot take into account space irregularities such as camber and ramp angle because of the two-dimensional limitations of beam theory. Thus the types of blades analyzed using this procedure is limited to low camber, high aspect ratio blades.

NASA Structural Analysis (NASTRAN) program was used to study the finite element modeling of blades as this program is coming into rather wide use. All modeling was done using a four-noded plate element (CQUAD) or a three noded triangular plate element (CTRIA). These elements have both inplane and bending stiffnesses that assumes a solid, constant thickness, homogeneous cross section. Energy theory applied to a polynomial distribution of displacement is used for the calculations. Transverse shear flexibility is included. Reference 2 provides a detailed theoretical discussion of the inverse power method of eigenvalue extraction used and the finite elements used in the analysis. Reference 3 describes the analysis procedure for the normal mode analysis.

To determine a correct modeling procedure for each method of analysis, flat plates with various aspect ratios were analyzed using an iterative modeling procedure. For the lumped mass analysis, the plates were modeled with an increasing number of constant property segments. Figures 1 and 2 illustrates how the results converge to a natural frequency using increasing number of segments. This would indicate the accuracy of the frequencies is a function of degrees of freedom of the model. This is verified by

Received July 31, 1974; revision received December 10, 1974.
Index categories: Structural Dynamic Analysis; Airbreathing Propulsion, Subsonic and Supersonic.

*Mechanical Engineer, Directorate of Propulsion and Power Engineering, Aeronautical Systems Division, USAF.